

Contribution from the Chemistry Department, University of Tasmania, Box 252C, Hobart, Tasmania 7001, Australia, and Fachbereich Chemie der Universität, 3550 Marburg/Lahn, Federal Republic of Germany

Temperature Dependence of the EPR Spectra of the Centers $\text{Cu}(\text{H}_2\text{O})_2\text{Cl}_4^{2-}$, $\text{Cu}(\text{NH}_3)_2\text{Cl}_4^{2-}$, and $\text{Cu}(\text{H}_2\text{O})(\text{NH}_3)\text{Cl}_4^{2-}$ in Cu^{2+} -Doped NH_4Cl : An Interpretation Using a Model of Dynamic Vibronic Coupling

Mark J. Riley,^{†‡} Michael A. Hitchman,^{*‡} Dirk Reinen,^{*§} and Gabriele Steffen[§]

Received September 17, 1987

The temperature dependence of the g tensors of the three centers *trans*- $\text{Cu}(\text{H}_2\text{O})_2\text{Cl}_4^{2-}$ (I), *trans*- $\text{Cu}(\text{NH}_3)_2\text{Cl}_4^{2-}$ (II), and *trans*- $\text{Cu}(\text{H}_2\text{O})(\text{NH}_3)\text{Cl}_4^{2-}$ (III), formed when Cu^{2+} is doped into NH_4Cl under different conditions, has been measured and interpreted by using a model in which the warped "Mexican hat" potential surface of a six-coordinate copper(II) complex is perturbed by a strain due to the inequivalence of the axial and in-plane ligands. The axially symmetric g tensors of centers II and III imply compressed tetragonal ligand coordination geometries, these being stabilized by the greater σ donor strength of the axial compared with the in-plane ligands. For center I the g values are significantly temperature dependent, and this is ascribed to higher order vibronic coupling forces, which dominate the tetragonal strain effect of the different ligands. For this center an orthorhombic g tensor is observed below ~ 12 K, but as the temperature is raised, the two higher g values are progressively replaced by an intermediate signal, so that above ~ 30 K the g tensor has effective tetragonal symmetry. The potential surface of this center has two minima, each corresponding to an orthorhombic coordination geometry involving short bonds to the water molecules and intermediate and long bonds to chloride ions. The two minima are distinguished by interchange of the intermediate and long bonds. Random lattice strain localizes the lowest vibronic wave function in one of the two wells, so that below ~ 12 K the signals of the individual orthorhombic complexes are resolved. When the temperature is raised, the thermal population of higher, more delocalized wave functions increases the rate of exchange between the wells, and when this becomes faster than the EPR time scale, the g values along the Cu-Cl bond directions are averaged. The potential surface of each center is strongly influenced by the balance between the tendency of the copper(II) to adopt an elongated tetragonal geometry due to the Jahn-Teller effect and the difference between the axial and in-plane metal-ligand σ -interactions, which favors a compressed tetragonal arrangement. The behavior of the centers is compared with that of other systems with similar and often also temperature-dependent geometries.

Introduction

The EPR spectrum of Cu^{2+} -doped NH_4Cl has been the subject of numerous studies,¹⁻¹² and it has been found that up to three distinct centers may be formed, depending upon the experimental conditions. The ENDOR measurements of Boettcher and Spaeth^{6,7} have established unequivocally that in two of these centers the Cu^{2+} ion occupies a facial interstitial site in the CsCl type unit cell of NH_4Cl (Figure 1). The charge compensation is accomplished by the substitution of two NH_4^+ ions by water molecules (center I) to give the complex *trans*- $\text{Cu}(\text{H}_2\text{O})_2\text{Cl}_4^{2-}$ or two ammonia molecules (center II) forming *trans*- $\text{Cu}(\text{NH}_3)_2\text{Cl}_4^{2-}$, as shown in Figure 1A,B. This is in agreement with the earlier conclusions drawn by Hagen and Trappeniers³ from the analysis of the hyperfine structure and supersedes the earlier interpretations of Pilbrow and Spaeth,² involving neighboring NH_4^+ vacancies, and the proposals of Bechtle et al.⁴ that the Cu^{2+} ions occupy off-center positions. Samples in which just one type of center predominates may be prepared by growing the crystals under acidic or basic conditions for I and II, respectively.³ Center III, which seems always to occur in conjunction with at least one of the other centers,^{2,3} has not been fully characterized in previous EPR investigations, though it was suggested on the basis of the optical spectrum¹³ that this involves the mixed complex *trans*- $\text{Cu}(\text{H}_2\text{O})(\text{NH}_3)\text{Cl}_4^{2-}$.

A phase transition occurs for NH_4Cl at 243 K,¹⁴ and this is accompanied by spectroscopic changes that have been discussed by several groups of workers.^{2,10} However, any consideration of the spectra in this temperature region must include the effects of the change in the bulk lattice constants, as well as any changes in the properties of the "guest" complexes. This fact, which has not always been appreciated, complicates the interpretation of the spectra considerably, and the present discussion will be restricted to temperatures below 230 K.

Between ~ 30 and 230 K the molecular g values of the three centers are rather similar, with g_{\parallel} close to 2, g_{\perp} in the range 2.2-2.3, and the anisotropy in the g tensor decreasing slightly as

the temperature rises. Early studies^{1,2} interpreted this as suggesting axially compressed ligand coordination geometries for all the centers, with ground states in which the unpaired electron is predominantly in the d_{z^2} orbital and the slight changes in the g values with temperature being due to vibronic effects. However, later studies^{4,6} showed that although the g tensor of center II remains essentially unaltered below ~ 30 K, that of center I changes from axial to orthorhombic symmetry, with one g value lying midway between the other two. On the basis of the ENDOR data, Boettcher and Spaeth⁷ proposed that the tetragonal-orthorhombic transition is related to the concerted "locking" of the hydrogen atoms of the two water molecules into the (110) crystal plane below ~ 30 K. At higher temperatures, the thermally activated reorientation of these ligands would occur by the "hopping" of the hydrogen atoms about the [001] axis. A major problem with this model, recognized by the authors, is that the reorientation of the ligands must occur in phase (i.e. they must remain coplanar) in order for the spectrum to become tetragonal. Moreover, the orientation of the hydrogen atoms affects only the π -bonding of the water molecules with the copper(II), and as the ground-state wavefunction is of σ -symmetry, this should have little influence on the EPR parameters or geometry of the complex. The model of Freeman and Pilbrow¹² postulating off-center positions of the Cu^{2+} ions in the " CuCl_4 " plane in the temperature range with an orthorhombic g tensor is in contradiction with the

* To whom correspondence should be addressed.

† Present address: Research School of Chemistry, Australian National University, GPO Box 4, Canberra, 2601, Australia.

‡ University of Tasmania.

§ Fachbereich Chemie der Universität Marburg.

- (1) Zaripov, M. M.; Chirkin, G. K. *Sov. Phys.—Solid State (Engl. Transl.)* **1964**, *6*, 1290.
- (2) Pilbrow, J. R.; Spaeth, J. M. *Phys. Status Solidi B* **1967**, *20*, 225, 237.
- (3) Hagen, S. H.; Trappeniers, N. J. *Physica (Amsterdam)* **1970**, *47*, 165.
- (4) Bechtle, B.; Boettcher, F.; Spaeth, J. M. *Phys. Status Solidi B* **1971**, *43*, K169.
- (5) Hagen, S. H.; Trappeniers, N. J. *Physica (Amsterdam)* **1973**, *66*, 166.
- (6) Boettcher, F.; Spaeth, J. M. *Phys. Status Solidi B* **1974**, *61*, 465.
- (7) Boettcher, F.; Spaeth, J. M. *Phys. Status Solidi B* **1974**, *62*, 65.
- (8) Watanabe, K.; Abe, H. *Phys. Status Solidi B* **1972**, *72*, 275.
- (9) Watanabe, K.; Abe, H. *J. Phys. Soc. Jpn.* **1975**, *38*, 755.
- (10) Kuroda, N.; Kawamori, A. *J. Phys. Chem. Solids* **1971**, *32*, 1233.
- (11) Billing, D. E.; Hathaway, B. J.; Tomlinson, A. A. G. *J. Chem. Soc. A* **1971**, *18*, 2839.
- (12) Freeman, T. E.; Pilbrow, J. R. *J. Phys. C* **1974**, *7*, 2365.
- (13) Stolov, A. L.; Yakovleva, Zh. S. *Sov. Phys.—Solid State (Engl. Transl.)* **1973**, *14*, 1810.
- (14) Perry, C. H.; Lownes, R. P. *J. Chem. Phys.* **1969**, *51*, 3648.

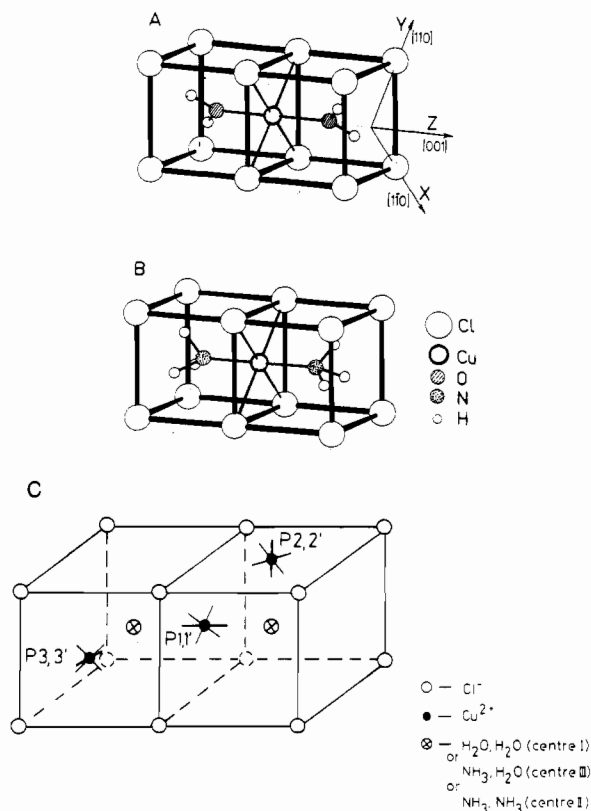


Figure 1. Copper(II) centers in the ammonium chloride lattice: (A) center I, $\text{Cu}(\text{H}_2\text{O})_2\text{Cl}_4^{2-}$; (B) center II, $\text{Cu}(\text{NH}_3)_2\text{Cl}_4^{2-}$; (C) orientation of the centers in the unit cell.

ENDOR measurements of Boettcher and Spaeth⁷ and will not be considered further. Watanabe and Abe⁹ explained the tetragonal-orthorhombic transition as due to a CuCl_4 coordination that is rhombically distorted at low temperatures, with two short and two long Cu-Cl bonds, becoming thermally averaged to a square plane at high temperatures. However, they postulated axial coordination by one NH_4^+ ion. The model to be presented in this paper is basically similar to that of Watanabe and Abe, but with axially coordinated water molecules; it must also be stressed that the "thermal averaging" describes a rapid exchange between two vibronic levels with orthorhombic geometries (plus the occupation of truly delocalized vibronic levels by a small fraction of the complexes) to give EPR parameters of tetragonal symmetry. This model is in accord with all experimental evidence on center I, in particular with the ENDOR data of Boettcher and Spaeth,⁷ and is also supported by EPR and structural results from various other compounds.

We recently reported a study of the temperature-dependent g values of Cu^{2+} -doped K_2ZnF_4 ,¹⁵ which was observed to have behavior quite similar to that reported for center II of Cu^{2+} -doped NH_4Cl . A theoretical model was developed in which the vibronic energy levels and wave functions were calculated within the framework of a Jahn-Teller potential with the addition of a lattice strain of tetragonal symmetry. The behavior of $\text{K}_2\text{Zn}[\text{Cu}]\text{F}_4$ could be explained satisfactorily in terms of a potential surface with a single minimum corresponding to a compressed octahedral ligand geometry. The electronic part of the ground state consisted predominantly of the d_{z^2} orbital, with a small component of $d_{x^2-y^2}$ mixed in by vibronic coupling, the temperature effects being caused by the thermal population of higher vibronic states. This model was subsequently extended to include the effects of an orthorhombic lattice strain and used to interpret the temperature-dependent g values of Cu^{2+} doped into a range of zinc hexahydrate complexes.¹⁶ Of particular relevance to the present problem is

the conclusion, first proposed by Reinen and Krause,¹⁷ that under certain conditions the superposition of an axially symmetric compression onto the cubic ligand field of a copper(II) complex can cause the most stable coordination geometry to have orthorhombic rather than the expected tetragonal symmetry.

The success of these treatments suggested that it would be of interest to apply the model to the Cu^{2+} -doped NH_4Cl centers, and the present paper reports the results of this investigation. The starting point of the model is the "warped Mexican hat" potential surface appropriate to a six-coordinate copper(II) complex in a cubic environment, this being perturbed by the equivalent of a lattice strain of tetragonal symmetry. In the doped ammonium chloride systems, the latter effect represents the inequivalence of the axial and in-plane ligands. An alternative treatment, similar to that described by Sorokin and Chirkin¹⁸ for the centers in Cu^{2+} -doped NH_4Br , is also discussed. Here, the starting point is the appropriate mixed-ligand complex of tetragonal symmetry, with vibronic coupling between the split states of the octahedral 2E_g ground state (a pseudo-Jahn-Teller effect) being considered in a second step.

Because of the cubic symmetry of the NH_4Cl host lattice, the study of the above three guest complexes provides a unique opportunity to investigate the factors influencing geometry and electronic structure of mixed-ligand copper(II) complexes in the absence of complicating factors such as cooperative interactions and low-symmetry lattice and ligand steric effects. It is inferred that the ratio of the axial to the in-plane ligand field, balanced against the natural tendency of Cu^{2+} to adopt an elongated tetragonal geometry, plays a dominant role in deciding the stereochemistry, and these ideas are discussed in relation to the structures observed for a number of pure copper(II) complexes. The experimental data available from previous studies have been supplemented by new measurements on center III and on center I in the temperature range over which the g tensor changes from orthorhombic to tetragonal symmetry. The latter spectra are shown to provide information on the rate of exchange between the two equivalent orthorhombic complexes that comprise this center and hence to the energy barrier to their interconversion.

Experimental Section

Sample Preparation. Pale blue cubic crystals ($\sim 1 \text{ mm}^3$) containing predominantly centers of type I were prepared by the method of Hagen and Trappeniers³ (sample 1). Blue crystals containing both centers I and III were grown in a similar manner, but by adding one drop of concentrated HCl instead of three to the growth solution (sample 2).

Measurement of the Spectra. A Varian E-15 spectrometer operating at X-band ($\sim 9.4 \text{ GHz}$) and Q-band ($\sim 35 \text{ GHz}$) was used for the EPR measurements. An Oxford Instruments liquid-helium flow cryostat was used for the measurements between 4 and 298 K, with the temperature being measured and controlled by using the standard accessory. Q-band experiments were performed at 4.2, 130, and 298 K. DPPH ($g = 2.0036$) was used as an internal standard.

The electronic absorption spectrum of a crystal containing center I was recorded over the range 2000–300 nm by using a Cary 17 spectrophotometer, the sample being cooled to $\sim 60 \text{ K}$ with a Cryodyne Model 22 closed-cycle refrigerator.

EPR Spectra of Centers I and III

The three different positions of the Cu^{2+} centers in the unit cell are P1, P2, and P3 in Figure 1C. The molecular z axis is defined parallel to the Cu-H₂O(NH₃) bond vectors, while x and y are oriented parallel to the Cu-Cl bond directions (Figure 1A,B). When there is an orthorhombic distortion these three positions split into six, because the long Cu-Cl bonds may occur in either the x or the y direction. Figure 2B shows Q-band EPR spectra measured with the magnetic field along [110], which is the x or y axis of polyhedron P1. When the temperature is lowered from 130 to 5 K, it may be seen that for center I the g_{\perp} signal of P1 splits into g_x and g_y components. The g_y component of P1 cannot be resolved directly, as it is obscured by the signals due to P2 and

(15) Riley, M. J.; Hitchman, M. A.; Reinen, D. *Chem. Phys.* **1986**, *102*, 11.
 (16) Riley, M. J.; Hitchman, M. A.; Wan Mohammed, A. *J. Chem. Phys.* **1987**, *87*, 3766.

(17) Reinen, D.; Krause, S. *Inorg. Chem.* **1981**, *20*, 2750.

(18) Sorokin, M. V.; Chirkin, G. K. *Sov. Phys.—Solid State (Engl. Transl.)* **1979**, *21*, 1720.

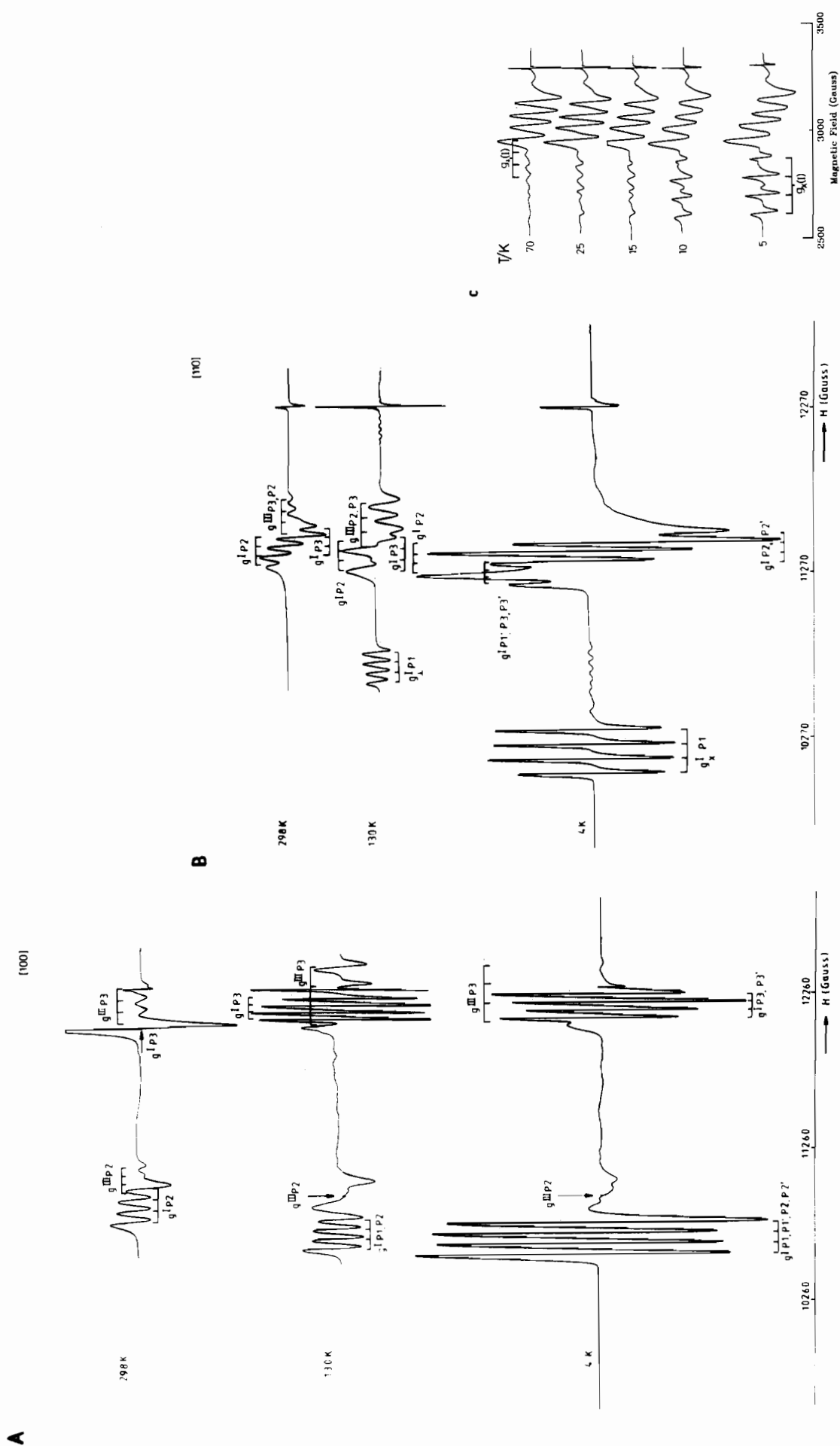


Figure 2. Temperature-dependent single-crystal EPR spectra (sample 1, crystal with almost entirely center I; sample 2, crystal with centers I and III): (A) sample 2 with the magnetic field parallel to the [100] direction measured at Q-band (the spectrum at 130 K was obtained by using a different crystal from those at 4 and 298 K, with a small misorientation of the crystal responsible for the deviation from ideal

behavior); (B) sample 2 with the magnetic field parallel to the [110] direction measured at Q-band (the spectrum at 130 K was obtained by using a different crystal from those at 4 and 298 K); (C) sample 1 with the magnetic field parallel to the [110] direction measured at X-band.

Table I. *g* and *A* Values of the Three Centers in NH₄Cl at Different Temperatures

<i>T</i> , K	center I ^a						center II ^b				center III ^a			
	<i>g</i> _x ^I	<i>g</i> _y ^I	<i>g</i> _z ^I	10 ⁴ <i>A</i> _x ^I , cm ⁻¹	10 ⁴ <i>A</i> _y ^I , cm ⁻¹	10 ⁴ <i>A</i> _z ^I , cm ⁻¹	<i>g</i> _⊥ ^{II}	<i>g</i> _∥ ^{II}	10 ⁴ <i>A</i> _⊥ ^{II} , cm ⁻¹	10 ⁴ <i>A</i> _∥ ^{II} , cm ⁻¹	<i>g</i> _⊥ ^{III}	<i>g</i> _∥ ^{III}	10 ⁴ <i>A</i> _⊥ ^{III} , cm ⁻¹	10 ⁴ <i>A</i> _∥ ^{III} , cm ⁻¹
4	2.410	2.185	2.019	98	53	50	2.220	1.996	73	240	2.237	2.010	55	108
130	2.292	2.292	2.019	67	67	43					2.239	2.010	54	116
298	2.256	2.256	2.045	79	79	15	2.209	2.0095	25	177.9	2.223	2.021	57	71

^aThis work. Estimated error limits: *g* values, ±0.003; *A* values, ±3 × 10⁻⁴ cm⁻¹. ^bLiterature data: Row 1, X-band.³ Error limits: *A*_∥, ±0.3 × 10⁻⁴ cm⁻¹; *A*_⊥, ±1 × 10⁻⁴ cm⁻¹; *g*_∥, ±0.0006; *g*_⊥, ±0.002. Row 3, K-band.⁶ Error limits: *A* values, ±3 × 10⁻⁴ cm⁻¹; *g* values, ±0.002.

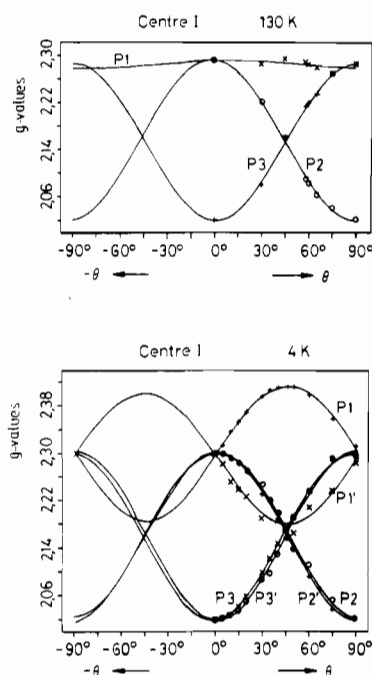


Figure 3. Angular dependence of the *g* tensor of center I with the magnetic field in the (100) plane. A small misorientation of the crystal is responsible for the deviation from ideal behavior.

P3, which occur at $(g_x + g_y + 2g_z)/4$. However, it can be obtained from the position of the latter signal, since both g_x and g_z can be measured directly. The orthorhombic-tetragonal transition of center I does not occur sharply and may also be somewhat sample dependent. For crystals containing almost entirely center I studied at X-band the orthorhombic signal was progressively replaced by a tetragonal one with this change occurring predominantly between ~12 and ~25 K (Figure 2C). Other crystals that contained center III in addition to center I (sample 2) were also studied at Q-band frequency. The spectra of these were better resolved with respect to the orthorhombic g_x and g_{\perp} components (Figure 2B). They showed a weak tetragonal signal even at 4.2 K (Figure 2B), while a weak orthorhombic signal could still be seen at 77 K. The fact that the orthorhombic and tetragonal spectra coexist is incompatible with the tetragonal spectrum simply being due to the motional narrowing of the orthorhombic spectrum of a set of identical complexes. However, as discussed below, the present model assumes that random lattice strains play an important role in the orthorhombic-tetragonal transition, and as these may vary within a sample, in this respect the complexes even within one crystal are not identical, so that a sharp orthorhombic-tetragonal transition is not expected. Strangely, the signals due to P1 could not be resolved at all at 298 K (Figure 2B). Possibly this is because of the phase transition that occurs at 243 K.

When the magnetic field is along the [100] direction, i.e. parallel to the *z* axis of P3, the spectra shown in Figure 2A are obtained. The angular dependence of the *g* tensor of center I is illustrated in Figure 3, and the temperature dependence of the principal *g* values of all three centers are shown in Figures 4 and 5. Data from the literature, particularly for center II, are included on the plots. The EPR data at three representative temperatures are summarized in Table I and, although these are not discussed in

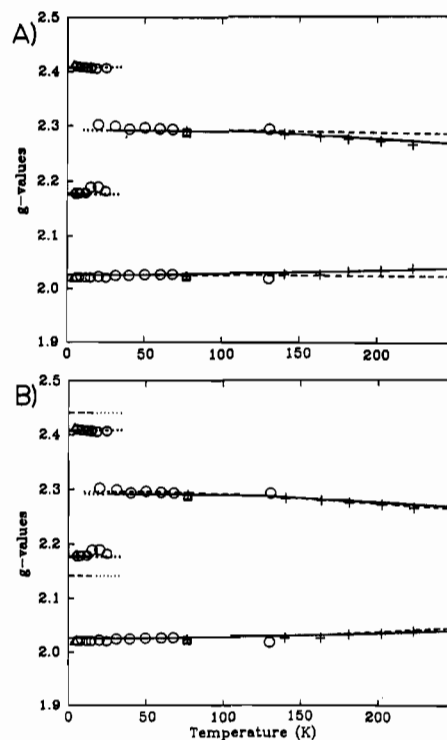


Figure 4. Calculated and experimental principal *g* values of center I. In each case $A_1 = 900$ cm⁻¹ and $h\nu = 210$ cm⁻¹. The different symbols indicate the source of the experimental data: (□) ref 2; (+) ref 5; (Δ) ref 6; (○) present study. Variables: (A) (—) $A_2 = 5.44$ cm⁻¹ ($\beta = 100$ cm⁻¹), $S_g = -200$ cm⁻¹ and $S_t = 1.5$ cm⁻¹, (---) $A_2 = 10.88$ cm⁻¹ ($\beta = 200$ cm⁻¹), $S_g = 600$ cm⁻¹, and $S_t = 1.5$ cm⁻¹; (B) (—) $A_2 = 5.44$ cm⁻¹ ($\beta = 100$ cm⁻¹), $S_g = -200$ cm⁻¹, and $S_t = 1.5$ cm⁻¹, (---) $A_2 = 5.44$ cm⁻¹ ($\beta = 100$ cm⁻¹), $S_g = -200$ cm⁻¹, and $S_t = 3.0$ cm⁻¹.

this paper, the Cu²⁺ hyperfine parameters are included in Table I for completeness.

Nature of Center III

While Pilbrow and Spaeth² and Hagen and Trappeniers³ reported limited experimental data on this center, the nature of the complex was not deduced. Crystals containing all centers are grown from nearby neutral aqueous ammoniacal solutions. Those that contain predominantly *trans*-Cu(H₂O)₂Cl₄²⁻ are obtained from slightly acid solution, while slightly basic solutions yield predominantly *trans*-Cu(NH₃)₂Cl₄²⁻.³ Since center III forms from a neutral or nearly neutral solution and always occurs in conjunction with one or both of the other centers, it seems very reasonable that it is the mixed complex *trans*-Cu(NH₃)(H₂O)Cl₄²⁻ as first proposed by Stolov et al.¹³ In agreement with this, center III has *g* values intermediate to those of the other two complexes (Table I). The temperature dependence of the *g* values of center III provides a useful test of the model used to explain the behavior of the other two centers as described below.

Properties To Be Explained by the Theoretical Model

The EPR spectra provide information on both the *g* values and hyperfine parameters of the centers. However, in the present study attention will be focused on just the *g* values. As has been pointed out elsewhere,¹⁶ the isotropic contribution to the metal hyperfine splittings may differ from one vibronic energy level to another

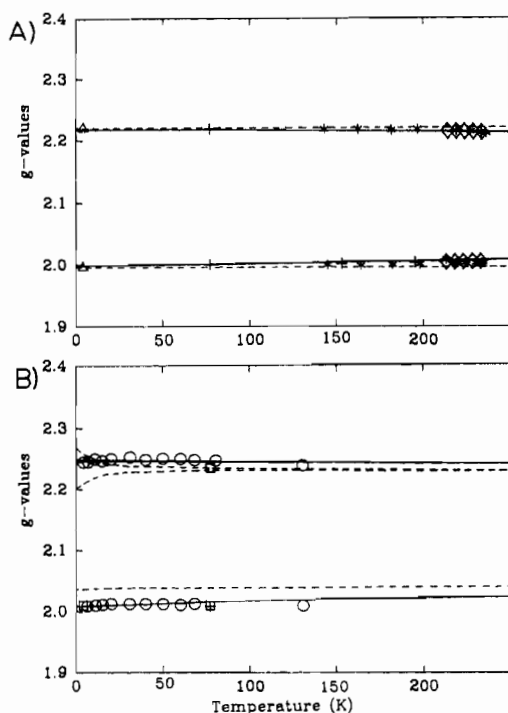


Figure 5. Calculated and experimental principal g values of centers II and III. The following parameters were used in the numerical calculations: $h\nu = 210 \text{ cm}^{-1}$, $A_1 = 900 \text{ cm}^{-1}$, $A_2 = 5.44 \text{ cm}^{-1}$ ($\beta = 100 \text{ cm}^{-1}$), $S_\epsilon = 1.5 \text{ cm}^{-1}$. The different symbols indicate the source of the experimental data: (\square) ref 2; ($*$) ref 10; ($+$) ref 5; (Δ) ref 6; (\diamond) ref 49; (\circ) present study. Variables: (A) center II (—) $S_\theta = -1200 \text{ cm}^{-1}$, (---) $S_\theta = -2000 \text{ cm}^{-1}$; (B) center III (—) $S_\theta = -600 \text{ cm}^{-1}$, (---) $S_\theta = -300 \text{ cm}^{-1}$.

in a way that is hard to predict, and this would greatly complicate the interpretation of these parameters.

The general features of the g tensors requiring explanation may be summarized as follows:

(i) At low temperature *trans*- $\text{Cu}(\text{H}_2\text{O})_2\text{Cl}_4^{2-}$ has highly orthorhombic g values, while the g tensors of both *trans*- $\text{Cu}(\text{H}_2\text{O})(\text{NH}_3)\text{Cl}_4^{2-}$ and *trans*- $\text{Cu}(\text{NH}_3)_2\text{Cl}_4^{2-}$ have tetragonal symmetry.

(ii) The EPR signals corresponding to the two higher g values of *trans*- $\text{Cu}(\text{H}_2\text{O})_2\text{Cl}_4^{2-}$ are gradually replaced by a single signal at an intermediate g value, which occurs continuously in the low-temperature region.

(iii) The slight convergence of g_{\parallel} and g_{\perp} , which occurs progressively as the temperature increases for all the complexes, becomes more pronounced along the series *trans*- $\text{Cu}(\text{NH}_3)_2\text{Cl}_4^{2-}$, *trans*- $\text{Cu}(\text{H}_2\text{O})(\text{NH}_3)\text{Cl}_4$, and *trans*- $\text{Cu}(\text{H}_2\text{O})_2\text{Cl}_4^{2-}$.

(iv) The deviation of g_{\parallel} from the value close to that of the free electron, which is predicted by a static model of a compressed octahedral Cu^{2+} complex, increases progressively along the series given above in section iii.

The model must also be consistent with the electronic spectra reported for centers I and II and with the bonding parameters and metal–ligand vibrational force constants appropriate for the various ligands.

Nature of the Model

The energy levels of the complexes will be considered by using the well-established model of a six-coordinate copper(II) complex perturbed by linear and nonlinear Jahn–Teller coupling and subject to a tetragonal strain caused by the inequivalence of the ligands. Details of this model, including the way in which the g values are calculated as a function of temperature, have been given elsewhere,^{15,16} so that only a brief account of the model will be presented here.

In a crystal lattice of cubic symmetry, the first order $E \otimes \epsilon$ vibronic coupling causes the potential surface of a copper(II) complex formed by six identical ligands to take the form of a “Mexican hat” as illustrated in Figure 6A. Here, the potential

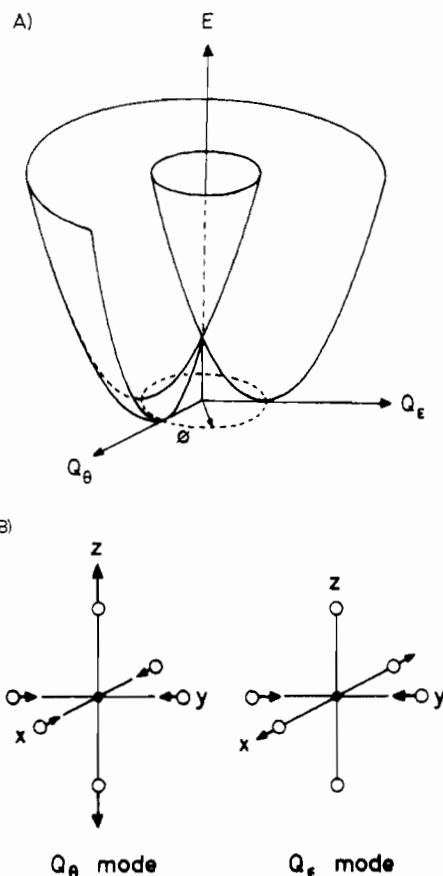


Figure 6. (A) Adiabatic “Mexican hat” potential surface of the linear $E \otimes \epsilon$ problem. (B) Tetragonal and orthorhombic components of the ϵ_g vibration of an octahedral complex.

energy is plotted as a function of the radial and angular parameters ρ and ϕ , which determine the components Q_θ , Q_ϵ of the doubly degenerate ϵ_g Jahn–Teller active vibrational mode (Figure 6B):

$$Q_\theta = \rho \cos \phi \quad Q_\epsilon = \rho \sin \phi \quad (1)$$

When higher order electronic terms and vibrational anharmonicity are taken into account, the minimum potential energy at ρ_0 becomes dependent on the angular coordinate, causing the perimeter of the Mexican hat to become “warped”. If the symmetry of the complex is lowered from cubic to tetragonal, either by crystal forces or, as in the present case, by the fact that two of the ligands are different from the other four, this can be taken into account by including a “strain” term in the calculations.

The Hamiltonian for the problem is that of the usual $E \otimes \epsilon$ Jahn–Teller coupling, H_{JT} , with the addition of the terms representing the strain, H_{ST} . The approximation is made that the strain does not destroy the symmetry of the cubic part of the Hamiltonian, so that there will be only one first-order and one second-order electronic coupling constant, and one harmonic vibrational force constant, instead of the six, nine, and two independent constants, respectively, which the low symmetry of the problem actually requires.¹⁶ Strictly speaking this approximation is valid only for strains that are a small perturbation to the cubic Hamiltonian. However, it has been found in previous studies^{15,16} that a meaningful model is obtained by using this approximation even when relatively large values of the strain are used. The form of the Hamiltonian is

$$H = H_{JT} + H_{ST}$$

$$H_{JT} = [(h\nu/2)(P_\theta^2 + P_\epsilon^2 + Q_\theta^2 + Q_\epsilon^2) + K_3 Q_\theta(Q_\theta^2 - 3Q_\epsilon^2)]I + A_1(Q_\theta\sigma_z - Q_\epsilon\sigma_x) + A_2[(Q_\theta^2 - Q_\epsilon^2)\sigma_z + 2Q_\theta Q_\epsilon\sigma_x]$$

$$H_{ST} = S_\theta\sigma_z - S_\epsilon\sigma_x \quad (2)$$

where

$$\sigma_x = \begin{pmatrix} 0 & 1 \\ 1 & 0 \end{pmatrix} \quad \sigma_z = \begin{pmatrix} 1 & 0 \\ 0 & -1 \end{pmatrix} \quad \mathbf{I} = \begin{pmatrix} 1 & 0 \\ 0 & 1 \end{pmatrix}$$

Here A_1 , A_2 , and K_3 are the first- and second-order coupling constants and the cubic anharmonicity of the Jahn–Teller active ϵ_g vibration, respectively. The energy of this vibration would be $h\nu$ in the complete absence of the Jahn–Teller effect. Both the coordinates and conjugate momenta in (2) and throughout this paper are in dimensionless form. These are related to the usual dimensioned quantities p , q by^{20,21}

$$P_i = \left(\frac{1}{mh\nu} \right)^{1/2} p_i \quad Q_i = \left(\frac{m\nu}{h} \right)^{1/2} q_i \quad (3)$$

Here m is the inverse of the G matrix element appropriate to the symmetry coordinates shown in Figure 6B, which would be the mass of one ligand in the case of an octahedral complex.²⁰ The parameters $h\nu$, A_1 , A_2 , K_3 , S_θ and S_ϵ of (2) are all in units of reciprocal centimeters but can be expressed in equivalent units if the dimensioned quantities in (3) are resubstituted into (2). Further discussion is given in the appendix of ref 15.

In the present problem, the inequivalence of the axial and in-plane ligands will remove the degeneracy of the ϵ_g vibration; this effect was investigated and found to be relatively unimportant, as discussed below. If the asymmetry in the π -bonding of the water ligands to the metal is neglected (and available experimental evidence suggests that this π -bonding is indeed effectively isotropic about the bond axis)¹⁹ the irregularity of the ligand field to be represented by the strain parameters S_θ and S_ϵ has tetragonal symmetry. However, the orthorhombic component of the strain S_ϵ is retained in the Hamiltonian in order to take into account the effects of small random lattice strains.

The desired energy levels and wavefunctions of the complexes are obtained by diagonalizing the matrix obtained by applying the above Hamiltonian (eq 2) to a truncated set of vibronic basis functions. This basis consisted of the two $E_g(d_{x^2-y^2}, d_{z^2})$ metal orbital wave functions and the $N [=1/2(n_\nu + 1)(n_\nu + 2)]$ two-dimensional harmonic oscillator wave functions of the ϵ_g vibration up to the level n_ν . Because of the strong coupling in these systems, the displacement in ρ is large, and a sizable basis set of vibrational wavefunctions is needed. In the present calculations a value of $n_\nu = 30$, corresponding to a vibronic basis size of 992 was found to provide a satisfactory convergence (this was tested by monitoring the effect of varying the basis size).

It is the second-order electronic and the anharmonic terms that discriminate between Q_θ and Q_ϵ and hence produce the "warped" Mexican hat potential surface.⁴⁶ Energy minima occur at $\phi = 0, 120, \text{ and } 240^\circ$ for $A_1, A_2 > 0$, corresponding to tetragonal elongations of the ligands along z , x , and y , and saddle points appear at $\phi = 60, 180, \text{ and } 300^\circ$, corresponding to tetragonal compressions. Because of its cubic dependence on ρ , the inclusion of the anharmonicity parameter K_3 in the calculations causes computational problems; the warping of the potential surface was therefore represented just by the second-order electronic term A_2 .¹⁶

Specification of the Parameters Used in the Calculations.
Energy of the Jahn–Teller-Active Vibration. In estimating this parameter, it is important to assess the effect that the inequivalence of the axial and in-plane ligands will have on the vibrational properties of the parent complexes in the absence of vibronic interactions. Taking the effective point group of each center to be D_{4h} , the degeneracy of the Jahn–Teller-active ϵ_g vibration of an octahedral copper(II) complex is removed, the two components transforming as modes of α_{1g} and β_{1g} symmetry. The energy and form of these were investigated by following procedures outlined by Cyvin²⁰ using valence force constants obtained from the vibrational frequencies reported for a number of related complexes of high symmetry. For G matrix elements²⁰ appropriate to the ligand masses, it was found²¹ that the energies of the α_{1g} and β_{1g}

components derived from the parent ϵ_g mode were ~ 225 and $\sim 197 \text{ cm}^{-1}$, respectively, justifying the approximation of a single Jahn–Teller coupling vibration of energy $h\nu = 210 \text{ cm}^{-1}$ used in the present calculations. Preliminary calculations confirmed that the splitting of the ϵ_g mode into two components has little effect on the EPR parameters of the complexes.^{21a}

While the approximation of a single vibrational energy is reasonable, it is noteworthy that the resulting tetragonal component of the ϵ_g mode will be mixed with the totally symmetric stretch of the complex. Calculations indicate²¹ that this coordinate is then one in which the axial ligands move six times the distance that the in-plane ligands move, though in an opposite direction, instead of twice the distance, as occurs in the Q_θ coordinate of an octahedral complex (Figure 6B).

Excited-State Energies. The electronic spectrum of center I was measured at 300 K by Billing et al.,¹¹ who reported peaks at 12 300, 11 000 (sh), and 9300 (sh) cm^{-1} . Very similar peak energies were observed in the spectrum measured at ~ 60 K in the present work: 12 500, 11 400 (sh), and 9300 (sh) cm^{-1} . The lowest energy peak is assigned to the transition between the split components of the 2E_g ground state of the parent octahedral complex, ΔE , while the higher energy pair of bands are transitions to the components of the excited ${}^2T_{2g}$ state. The spectrum of center II has been measured by Billing et al.¹¹ and Kuroda and Kawamori,¹⁰ the reported band maxima being very similar: $\sim 14 000$ and 9500 (sh) cm^{-1} . Again, the lower energy peak is assigned as ΔE , and the higher band is assigned to the unresolved components of the split ${}^2T_{2g}$ state. The original assignment of Kuroda and Kawamori¹⁰ differs from that presented here in that they placed one of the transitions to the split ${}^2T_{2g}$ state at $\sim 40 000 \text{ cm}^{-1}$; this seems untenable, as it implies quite unreasonable bonding parameters in the complex. For center III, transition energies intermediate between those of I and II have been observed.¹³

Linear Coupling Constant A_1 . This is related to the Jahn–Teller stabilization energy E_{JT} by the expression⁴⁶

$$A_1 = (2h\nu E_{JT})^{1/2}$$

where $h\nu$ is the energy of the Jahn–Teller active vibration. The Jahn–Teller stabilization energy may be obtained from ΔE :

$$\Delta E \approx 4E_{JT} + 2|S_\theta|$$

Substituting the values of $\Delta E \approx 9500 \text{ cm}^{-1}$ and $h\nu \approx 210 \text{ cm}^{-1}$ and anticipating a value of the strain parameter $S_\theta \approx -1000 \text{ cm}^{-1}$ suggest a linear coupling constant $A_1 \approx 900 \text{ cm}^{-1}$ for each of the centers.

Second-Order Coupling Constant A_2 . In the present approach this parameter defines the barrier height, 2β , between the equivalent wells of the warped Mexican hat potential surface along the Jahn–Teller radius ρ_0 and is given approximately by

$$\beta \approx A_2\rho_0^2$$

It is generally recognized that the value of β is hard to define, and previous estimates for related complexes have been in the range $\beta \approx 50\text{--}350 \text{ cm}^{-1}$ ($A_2 = 2.72\text{--}19.04 \text{ cm}^{-1}$).^{15,16} Within these limits, this parameter was therefore taken as a free variable in the present calculations.

Lattice Strain Parameters. In the present calculations the strain parameter S_θ is defined by the energy difference δE between the d_{z^2} and $d_{x^2-y^2}$ orbitals in the parent mixed-ligand complex with metal–ligand bonds appropriate for a regular octahedral geometry:

$$\delta E = 2S_\theta$$

Thus, in center I, S_θ is a measure of the difference in σ -bonding

(19) Hitchman, M. A.; Waite, T. D. *Inorg. Chem.* **1976**, *15*, 2150.

(20) Cyvin, S. J. *Molecular Vibrations and Mean Square Amplitudes*; Elsevier: Amsterdam, 1968.

(21) (a) Riley, M. J. Ph.D. Thesis, University of Tasmania, 1987. (b) Cohen-Tannoudji, C.; Dui, B.; Lahoe, F. *Quantum Mechanics*; Wiley: New York, 1977; pp 487–8; (c) Wagner, M. In *The Dynamic Jahn–Teller Effect in Localised Systems*; Perlin, Yu. E., Wagner, M., Eds.; North Holland: Amsterdam, 1984; pp 159–60.

(22) Lupei, A.; McMillan, J. A. *Rev. Roum. Phys.* **1973**, *18*, 437.

power between the H_2O and Cl^- ligands, while in center II, it represents the difference between NH_3 and Cl^- . Again, the strain parameters were taken as free variables, though they should be consistent with the known bonding parameters of the ligands. It is therefore expected that the σ -bonding power follows the sequence $\text{Cl}^- < \text{H}_2\text{O} < \text{NH}_3$, implying that S_θ is negative. It should also be noted that if the assumption that center III is the mixed complex $\text{Cu}(\text{H}_2\text{O})(\text{NH}_3)\text{Cl}_4^{2-}$ is correct, S_θ should have a value approximately midway between those of the other two centers.

In the calculations pertinent to center I, in which the strain generates two equivalent minima in the potential surface, the effects of the random lattice strains that discriminate between the minima for each individual complex must be included. This was done by including an orthorhombic strain parameter $S_\epsilon = 1.5 \text{ cm}^{-1}$. The value is similar to those proposed for the random strain in other doped $\text{Cu}(\text{II})$ complexes.²³ In fact, a range of strain energies will be present in any one crystal, so that the chosen value represents an average. Since relatively sharp EPR signals are observed at low temperature, the calculated g values must be relatively insensitive to the value of the random strain, and this was tested by repeating the calculations using the value $S_\epsilon = 3.0 \text{ cm}^{-1}$ (Figure 4B).

Calculation of the g Values. Except for center I in the low-temperature range where an orthorhombic g tensor was observed the g values were calculated by the method described in detail elsewhere.¹⁶ This procedure involves calculating the g values of each vibronic level from the electronic part of its wave function, after having included the effects of spin-orbit coupling with the excited electronic states. The g values of each complex were then obtained by averaging the values of the individual vibronic levels, using weighting factors given by a Boltzmann distribution. This process was carried out at a sufficient number of temperatures to generate curves for comparison with the experimental data. This method is only appropriate for those situations where the rate of exchange between the vibronic levels is more rapid than the EPR time scale. As discussed below, when the orthorhombic g tensor is observed for center I, it is thought that this is associated with individual levels that are localized in either of the two wells in the potential surface of this complex, i.e. that the rate of exchange between the wells is slower than the EPR time scale. In this case, therefore, the g values are not a Boltzmann average of the individual vibronic levels.

Potential Surfaces, Ground-State Wave Functions, and Geometries of the Centers. The potential surfaces and vibronic wave functions of the complexes were estimated by comparing the calculated g values with those observed experimentally. Covalency was taken into account by using orbital reduction factors, and the isotropic values $k = 0.81$ and 0.84 were found to satisfactorily reproduce the g values of centers II and III, respectively. In the case of center I, it was found that the experimental values could not be reproduced satisfactorily by using an isotropic orbital reduction parameter. However, the values $k_x = k_y = 0.9$ and $k_z = 0.7$ fit the data well.

As discussed above, a value of $A_1 = 900 \text{ cm}^{-1}$ was assumed for the linear coupling constant and the energy of the harmonic vibration (the ϵ_g vibration of the hypothetical "cubic" $\text{CuX}_2\text{Cl}_4^{2-}$ species) was taken as 210 cm^{-1} for all of the centers. In determining the optimum values of the warping and strain parameters of each complex, it was convenient to first consider the low-temperature g values, as these only required the calculation of the lowest vibronic level. The temperature dependence of the g values was then used to "fine-tune" the possible range of each pair of parameters. It may be noted that the g_z values of the tetragonal centers II and III require the dynamic mixture of $\sim 1\%$ and $\sim 5\%$ $d_{x^2-y^2}$ character in the predominantly d_{z^2} ground vibronic state, respectively, while the orthorhombic g values of center I provide a strong constraint to the positions of the minima in the potential surface of this complex. In addition, the nature of the orthorhombic-tetragonal transition implies a barrier height of < 100

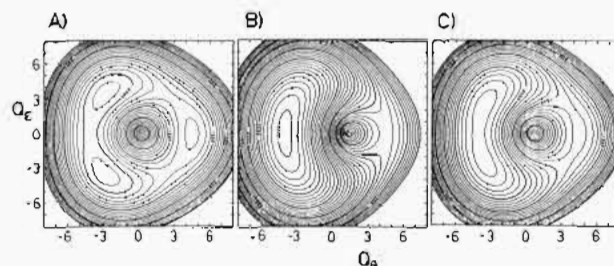


Figure 7. Contour plots of the lower adiabatic surfaces for the "best-fit" parameters: $h\nu = 210 \text{ cm}^{-1}$, $A_1 = 900 \text{ cm}^{-1}$, $A_2 = 5.44 \text{ cm}^{-1}$ ($\beta = 100 \text{ cm}^{-1}$), and $S_\epsilon = 1.5 \text{ cm}^{-1}$; $S_\theta = -200 \text{ cm}^{-1}$ (center I), $S_\theta = -1200 \text{ cm}^{-1}$ (center II), or $S_\theta = -600 \text{ cm}^{-1}$ (center III). The potentials of centers I-III are shown in parts A-C, respectively; the contour interval is 100 cm^{-1} .

cm^{-1} between the orthorhombic minima in the potential surface of center I (see below).

The behavior of center I provided far more stringent constraints than did that of II or III, so this was used to estimate optimum values of β and S_θ initially. Following this it was found that the g values of the other two centers could be reproduced satisfactorily by assuming a value of β identical with that of center I and unique values of S_θ . The optimum estimates of the strain parameters of the centers were found to be -200 , -1200 , and -600 cm^{-1} for centers I, II, and III, respectively. The sensitivity of the calculated g values to the values of the strain and the warping parameter β is illustrated in the plots shown in Figures 4 and 5. It may be seen from the curves in Figure 4A that the g values calculated for center I by using the parameters $\beta = 100 \text{ cm}^{-1}$ and $S_\theta = -200 \text{ cm}^{-1}$ agree with experiment somewhat better than those calculated by using $\beta = 200 \text{ cm}^{-1}$ and $S_\theta = -600 \text{ cm}^{-1}$, particularly at higher temperature. However, as is shown in Figure 4B, with very low values of β , the g values become rather sensitive to the value of the random strain in the low-temperature region. Since a range of values of the random strain are likely to be present in any sample, this might imply broader EPR signals than are observed experimentally. It thus seems unlikely that β is less than $\sim 100 \text{ cm}^{-1}$. It was found that it was not possible to simultaneously reproduce the higher temperature ($> 30 \text{ K}$) behavior of center I and also have the two lowest vibronic functions completely localized in separate wells. This inadequacy of the model is possibly due to the fact that a cubic form is assumed for the warping term in the Hamiltonian (eq 2) although the actual symmetry of the mixed-ligand complex is only tetragonal. As may be seen from the plots in Figure 5A,B, the value of S_θ may be determined quite accurately for center III but much less precisely for center II.

The lower adiabatic potential surfaces of the centers were calculated by diagonalizing the vibronic Hamiltonian with respect to the potential energy operator using the above optimum parameters. Contour plots of the lower potential surfaces of the centers are shown in Figure 7. The variation of the energy as a function of the relative displacement in the two components of the ϵ_g mode, as specified by the angle ϕ measured at the Jahn-Teller radius ρ_0 of the energy minimum, is shown for each center in Figure 8. Because the "warped Mexican hat" potential surfaces of the centers do not have circular symmetry, the plots in Figure 8 do not accurately represent the "path of least energy" around the minima. However, they do allow a ready comparison of the important features of the centers. The five lowest energy levels of each center are also shown in Figure 8, and the vibrational and electronic wave functions associated with each level of center I are illustrated in Figure 9.

The potential of center I has two well-developed minima (Figure 8A), and the vibrational probability plots associated with these (Figure 9) correspond to displacements in the orthorhombic component of the ϵ_g mode (Figure 6B), which are opposite in sign and almost equal in magnitude. The "inversion splitting" and random strain make the two lowest vibronic levels slightly different in energy (by 3 cm^{-1}) and localizes the wave functions in each

(23) Reynolds, R. W.; Boatner, L. A.; Abraham, M. M.; Chen, Y. *Phys. Rev. B: Solid State* 1974, 10, 3802.

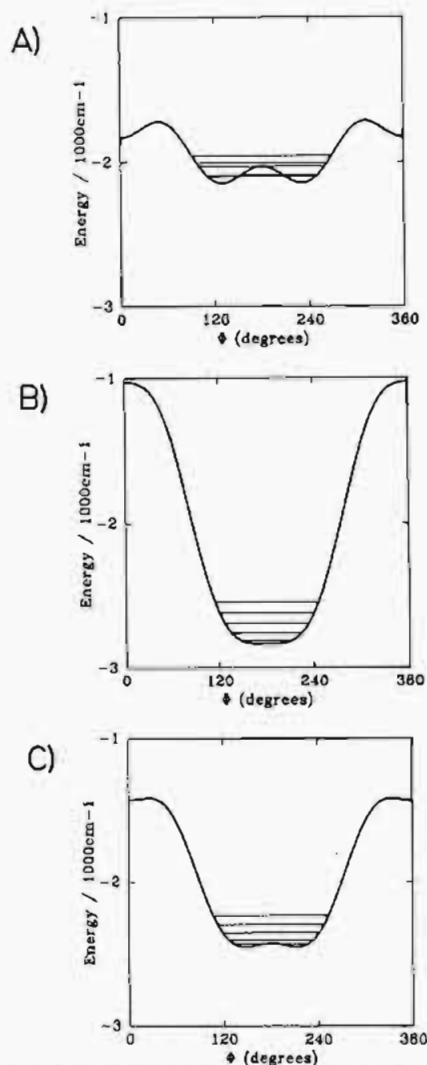


Figure 8. Circular cross section along the angular coordinate at the radius $\rho_0 (=A_1/h\nu)$ of the potential surfaces shown in Figure 7. The five lowest energy levels are also shown after having subtracted the zero-point energy of the radial vibration.

well. The electronic part of the lowest wave function at this static geometry is

$$0.97d_{z^2} + 0.24d_{x^2-y^2} \quad (4)$$

from which it might be thought that the center in this state has an essentially compressed tetragonal ligand geometry with a mainly d_{z^2} ground state. In fact, in agreement with the orthorhombic nature of the g values, the geometry is orthorhombic, almost midway between elongated (along x) and compressed (along z) tetragonal ligand arrangements, as may be seen by inspecting the respective ground states in the limiting conformations: $d_{z^2-y^2} = 3^{1/2}d_{z^2}/2 + 1/2d_{x^2-y^2}$ and d_{z^2} . The wave function (eq 4) has the largest lobe along z , the intermediate lobe along y , and the smallest lobe along x , with the corresponding short, medium, and long bonds being to water molecules and two pairs of chloride ions. The wave function with the slightly higher energy has an essentially identical form (and g tensor) except for an interchange of the x and y axes (Figure 9; this wave function corresponds to that in (4) with a negative sign connecting the functions). Because of the small energy difference between the levels, both will be substantially thermally populated even at 4.2 K. The fact that individual EPR signals are observed for the levels at this temperature therefore shows that the rate of exchange between them is slower than the frequency difference between their resonances. It must also be remembered that because the strain is random, an equal number of centers will occur with $S_0 = -1.5 \text{ cm}^{-1}$, rather than $+1.5 \text{ cm}^{-1}$, and these will have the relative energies of the two

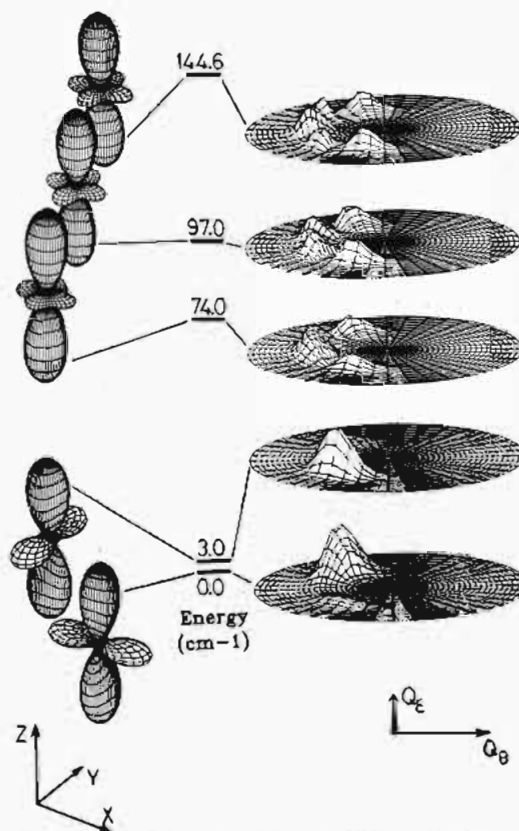


Figure 9. Probability plots of the electronic (left) and vibrational (right) parts of the five lowest vibronic levels of center I.

lowest levels reversed. The next highest level, at 74 cm^{-1} , is almost completely delocalized over the two wells, as are the other wave functions at still higher energy. It is presumably the thermal population of these levels that provides the pathway by which the exchange between the two lowest levels increases as the temperature rises. It is gratifying to note that the energy of the lowest delocalized level agrees well with the analysis of the orthorhombic-tetragonal change in the spectrum (see below). It is also the thermal population of the higher vibronic levels that causes the slight convergence of the g_{\parallel} and g_{\perp} values at higher temperatures (Figure 5). The third minimum at $\phi = 0^\circ$, corresponding to a $d_{z^2-y^2}$ wave function, is too high in energy to significantly affect the g values at the temperatures under consideration (Figure 8A). The high energy of this minimum is related to the fact that it corresponds to long bonds along z , which are directed toward the strongest ligands, the water molecules.

The potential surface of center II has a single minimum at $\phi = 180^\circ$, corresponding to a compressed tetragonal ligand geometry with an almost pure d_{z^2} ground state (Figure 8B). The slight convergence of the g values of this complex as the temperature rises (Figure 5A) is due to the thermal population of higher vibronic levels, which have a progressively greater contribution of the $d_{z^2-y^2}$ wave function. Within the framework of the present model, the temperature dependence of this center is caused by the vibronic coupling mechanism discussed originally by O'Brien²⁴ and amplified more recently to describe the behavior of Cu²⁺-doped K_2ZnF_4 .¹⁵ For *trans*-Cu(NH₃)₂Cl₄²⁻ the energy of the so-called "angular vibration", which is actually the octahedral Q_2 mode at ρ_0 , is $\sim 65 \text{ cm}^{-1}$ (Figure 8B). It is this mode that is responsible for the change from tetragonal to orthorhombic geometry in center I, so it is not surprising that it is soft in nature. Its energy is quite similar to that deduced for the CuF₆⁴⁻ centers in $K_2Zn[Cu]F_4$.¹⁵

In agreement with its formulation as a mixed complex, the potential surface of center III is intermediate between those of

the other two centers (Figure 7C). Although a double minimum is present, this is so shallow that it lies below the lowest vibronic energy level. The ground-state wave function is completely delocalized, and the electronic part is predominantly d_{z^2} , though with a substantial contribution ($\sim 5\%$) of $d_{x^2-y^2}$. It is this latter contribution that produces the significant deviation of g_z (2.01, Figure 5B) from the value expected for a pure d_{z^2} orbital at 4.2 K (~ 1.98). The convergence of the g values that occurs as the temperature rises is again due to the thermal population of higher vibronic levels, which have increasing contributions from the $d_{x^2-y^2}$ orbital. However, it should be noted that the unusual shape of the potential surface means that the change is significantly less than would be expected for an approximately harmonic "angular" vibration in the vibronic coupling model of O'Brien.^{15,24}

Orthorhombic \rightarrow Tetragonal Transition in Center I. For this center, as the temperature rises from 4 K, the signals associated with g_x and g_y broaden and are gradually replaced by a signal corresponding to an intermediate g value (Figure 2B,C). This behavior is reminiscent of the tetragonal \rightarrow isotropic transition observed in the EPR spectrum of the $\text{Cu}(\text{H}_2\text{O})_6^{2+}$ complex in Cu^{2+} -doped $\text{Zn}(\text{H}_2\text{O})_6\text{SiF}_6$, which also occurs over a comparable temperature range. The mechanism for the latter transition has been investigated by several groups of workers.²⁵ The x , y , and z molecular axes are crystallographically equivalent in the zinc host complex. However, it has been suggested that random lattice strains make the ligands of each guest copper(II) complex slightly inequivalent, and this has the effect of localizing the lowest vibronic wave functions in the three wells in the potential surface of each complex. At low temperature, the rate of exchange is slow, so that the observed spectrum is the superposition of the spectra of a random distribution of complexes, each localized in one of the three wells characterized by a tetragonal g tensor. At higher temperatures, the rate of exchange between the wells increases, and an averaged g tensor is observed.

A basically similar mechanism is proposed for the transition in the EPR spectrum of *trans*- $\text{Cu}(\text{H}_2\text{O})_2\text{Cl}_4^{2-}$, except that here two, rather than three, wells in the potential surface are involved (see Figure 9A). Because the dynamics is essentially two-dimensional, we have proposed that processes of this kind be called "planar-dynamic".²⁶ For each complex, random lattice strains were represented in the present calculations by an orthorhombic component, $S_z = 1.5 \text{ cm}^{-1}$, and this has the effect of localizing the lowest vibronic wave functions largely in one of the two wells, the energy separation between these being 3 cm^{-1} . It is suggested that at low temperature the rate of exchange between the wells is slow on the EPR time scale, so that the signals associated with the individual vibronic wave functions of orthorhombic symmetry may be resolved. As the temperature is raised, thermal population of higher levels, which are delocalized (Figures 8a and 9), allows rapid exchange between the wells. As the two lowest wave functions only differ by the interchange of the x and y molecular axes, just the EPR signals associated with these directions become averaged, yielding a tetragonal g tensor.

It is impossible to treat the exchange mechanism rigorously, since the spectra in the temperature region of interest are poorly resolved (Figure 2C); moreover, as has already been mentioned, the temperature range over which the coalescence occurs is apparently somewhat sample dependent. However, a semiquantitative investigation was carried out, and although the results will not be presented here, it was found²¹ that the essential features of the change in the spectra could be reproduced satisfactorily by assuming an activation energy for the exchange process of $\sim 75 \text{ cm}^{-1}$. As the activation energy presumably represents the energy of the lowest vibronic level, which is delocalized over the two wells, this value agrees well with the estimate of 74 cm^{-1} obtained in the above calculations (Figure 9).

Discussion of the Strain Parameters. In the present model the strain parameters represent the difference in σ -bonding power

between the axial and in-plane ligands in the parent *trans*- $\text{CuX}_2\text{Cl}_4^{2-}$ complexes. Both NH_3 and H_2O are expected to be stronger σ -donors than Cl^- , so that the ligand field asymmetry tends to favor a compressed tetragonal geometry for each complex. When $\text{X} = \text{NH}_3$, the strain is large enough to stabilize a compressed tetragonal geometry. However, when $\text{X} = \text{H}_2\text{O}$ the balance between the ligand field effects and the natural tendency of copper(II) to prefer an elongated tetragonal geometry (quantified in the model by β) means that a compromise between the opposing forces occurs, resulting in an orthorhombic geometry. For center III, the opposing effects are so delicately balanced that although a compressed tetragonal geometry occurs, this is only marginally stable with respect to distortion toward an orthorhombic ligand arrangement.

Clearly, an important test that the model is realistic is provided by a comparison of the "best-fit" strain parameters with bonding parameters derived from the spectra of simple model copper(II) complexes. The planar $\text{Cu}(\text{II})$ complexes formed by the relevant ligands form a suitable set for comparison.

For planar $\text{Cu}(\text{NH}_3)_4^{2+}$ the transition $d_{xy} \rightarrow d_{x^2-y^2}$ occurs at 20700 cm^{-1} ,²⁷ and the simple angular overlap model of the bonding in metal complexes²⁸ equates this to $3e_\sigma(\text{NH}_3)$, where $e_\sigma(\text{NH}_3) \approx 6900 \text{ cm}^{-1}$ represents the σ -antibonding power of one ammonia ligand. For planar CuCl_4^{2-} a similar analysis of the transition energies,²⁹ taking into account the small π -interaction of the chloride ions, yields the estimate $e_\sigma(\text{Cl}^-) \approx 5330 \text{ cm}^{-1}$. This implies that the difference in σ -antibonding power is $e_\sigma(\text{NH}_3) - e_\sigma(\text{Cl}^-) \approx 1570 \text{ cm}^{-1}$ at the bond distances appropriate to the planar complexes. A simple calculation³⁰ suggests that this would be reduced by $\sim 33\%$ to $\sim 1000 \text{ cm}^{-1}$ in the corresponding hypothetical regular octahedral complex, in good agreement with the estimate of $S_\theta \approx -1200 \text{ cm}^{-1}$ obtained from the above analysis of the EPR data.

The planar, four-coordinate $\text{Cu}(\text{H}_2\text{O})_4^{2+}$ ion has not as yet been prepared, but the electronic spectrum of four-coordinate *trans*- $\text{Cu}(\text{H}_2\text{O})_2\text{Cl}_2$ shows peaks due to the transitions d_{xy} and $d_{xy,yz} \rightarrow d_{x^2-y^2}$ at 13200 and 15200 cm^{-1} , respectively.³¹ Allowing for the π -bonding effect of the ligands results in an average value $e_\sigma(\text{Cl}^-, \text{H}_2\text{O}) \approx 5730 \text{ cm}^{-1}$, which implies $e_\sigma(\text{H}_2\text{O}) \approx 500 \text{ cm}^{-1}$ at octahedral bond distances, in fair agreement with the "best-fit" estimate of $\sim 200 \text{ cm}^{-1}$ from the EPR analysis.

The formulation of center III as *trans*- $\text{Cu}(\text{H}_2\text{O})(\text{NH}_3)\text{Cl}_4^{2-}$ implies a bonding difference between the axial and in-plane ligands halfway between those of the other two centers. The "best-fit" estimate of $\sim 600 \text{ cm}^{-1}$ from the EPR analysis agrees well both with the average of the other estimates, $\sim 600 \text{ cm}^{-1}$, and with the difference in the bonding parameters derived from optical spectra, $\sim 750 \text{ cm}^{-1}$.

Comparison of the Geometries of the "Guest" Complexes with Those of Other Copper(II) Compounds. It is interesting to compare the geometries deduced for the three centers of Cu^{2+} -doped NH_4Cl with those observed for pure complexes with analogous stoichiometries. Isolated $\text{Cu}(\text{H}_2\text{O})_2\text{Cl}_4^{2-}$ units having very similar geometries are present in $\text{K}_2\text{CuCl}_4 \cdot 2\text{H}_2\text{O}$ ³² and $(\text{NH}_4)_2\text{CuCl}_4 \cdot 2\text{H}_2\text{O}$,³³ involving short bonds to the two water molecules and two of the chloride ions and longer bonds to the remaining two chloride ions ($\text{Cu}-\text{O} = 197.1$ and 195.4 pm ; $\text{Cu}-\text{Cl} = 228.5$ and 227.1 pm and 289.5 and 297.1 pm for the two compounds, respectively). A very similar orthorhombic coordination geometry is observed for $\text{CuCl}_2 \cdot 2\text{H}_2\text{O}$,³⁴ though here the chloride ligands bridge between the copper(II) ions, forming an infinite two-dimensional lattice. These pure complexes thus have coordination geometries quite

(27) Schneider, W.; Baccini, P. *Helv. Chim. Acta* **1969**, *52*, 1955.

(28) Schaffer, C. E. *Pure Appl. Chem.* **1970**, *24*, 361.

(29) Hitchman, M. A.; Cassidy, P. *Inorg. Chem.* **1978**, *17*, 1682.

(30) Hitchman, M. A. *Inorg. Chem.* **1982**, *21*, 821.

(31) McDonald, R. G.; Hitchman, M. A., to be submitted for publication.

(32) Chidambaram, R.; Navarro, Q. O.; Garcia, A.; Linggoatmodjo, K.; Shi-Chien, L.; Suh, I.; Sequeira, A.; Srikanta, S. *Acta Crystallogr., Sect. B: Struct. Crystallogr. Cryst. Chem.* **1970**, *B26*, 827.

(33) Bhakay-Tamhane, S. N.; Sequeira, A.; Chidambaram, R. *Acta Crystallogr., Sect. B: Struct. Crystallogr. Cryst. Chem.* **1980**, *B36*, 2925.

(34) Engberg, A. *Acta Cryst. Scand.* **1970**, *24*, 3510.

(25) Dang, L. S.; Buisson, R.; Williams, F. I. B. *J. Phys. (Paris)* **1974**, *35*, 49.

(26) Reinen, D.; Friebel, F. *Struct. Bonding (Berlin)* **1979**, *37*, 1.

consistent with that deduced for center I in the present study. However, even at room temperature cooperative interactions between the complexes, which are not present in the doped NH₄Cl systems, act to stabilize just one of the two possible orthorhombic geometries in the pure copper(II) compounds.

Isolated Cu(NH₃)₂Cl₄²⁻ units occur in several compounds,^{35,36} and in marked contrast to the analogous aqua complexes these have axially symmetric compressed geometries with short bonds to the two ammonia molecules (Cu–N ≈ 195 pm) and long bonds to the four chloride ions (Cu–Cl ≈ 276 pm). This matches well with the geometry of the host site for Cu²⁺ (center II) in NH₄Cl, where Cu–Cl spacings of 274 pm and Cu–N bond lengths of 194 pm are implied if the NH₃ ligands substitute directly for NH₄⁺ ions in the unit cell and the dimensions of this are unaltered by the substitution.³⁷ Our theoretical model rationalizes the unusual stereochemistry of this complex as being caused by the strong axial compression of the ligand field, which in this case is sufficient to overcome the natural tendency of the metal ion to adopt an elongated tetragonal geometry (nonlinear Jahn–Teller interaction).

The present study concludes that center III is the mixed complex Cu(NH₃)(H₂O)Cl₄²⁻ and that this also has an axially compressed geometry. As far as we are aware, no copper(II) compound containing this species is known, so comparison with the geometry of a pure complex is not feasible.

Description of the Centers in Terms of Tetragonal Complexes Perturbed by Pseudo-Jahn–Teller Coupling

An alternative treatment that could be used to interpret the behavior of each center is that of a complex of compressed *D*_{4h} symmetry or, in the case of center III, *C*_{4v} symmetry, perturbed by a pseudo-Jahn–Teller vibronic interaction between the ²A_{1g}(z²) ground state and ²B_{1g}(x² – y²) excited state. An approach of this kind was used by Sorokin and Chirkin¹⁸ to explain the nature of the two centers formed when Cu²⁺ is doped into NH₄Br, which exhibit a behavior analogous to that of centers I and II in NH₄Cl. The active mode is the in-plane stretch of β_{1g} (or β₁) symmetry directly analogous to the orthorhombic component *Q*_t (Figure 6b) of the Jahn–Teller active mode of a copper(II) complex with six identical ligands. Strong vibronic coupling can produce a ground-state potential surface having double minima displaced symmetrically on either side of the origin of the β_{1g} normal coordinate; this corresponds to the situation observed experimentally for center I. Weaker coupling, caused by the larger separation of the ²A_{1g}(z²) and ²B_{1g}(x² – y²) states at the equilibrium tetragonal geometry of centers II and III, leaves the basic form of the potential surface unaltered but induces an admixture of ²B_{1g}(x² – y²) into the ground state. This model has the merit of simplicity, involving three unknown parameters: the vibronic coupling coefficient, the energy of the coupling mode and the energy separation of the two electronic states at the relaxed geometry along the α_{1g} tetragonal coordinate.

A preliminary investigation of the three NH₄Cl centers was in fact carried out by using this model in the present study.²¹ Although it was found that qualitative agreement could be obtained with the observed data, it was not possible to satisfactorily reproduce both the temperature dependence and the magnitudes of the *g* values of centers I and III simultaneously. While it appeared likely that agreement with experiment could be improved by including an anharmonicity term in the parameterisation of the β_{1g} vibration, this approach was not pursued further. Although the model of Sorokin and Chirkin provides a way of interpreting the properties of the centers in terms of vibronic coupling, which is just as valid as that described in the preceding sections, in our view it suffers from the disadvantage that the physical significance of the coupling and anharmonicity coefficients is much less clear than is the case with the model used in the present paper.

General Conclusions and Comparison with Other Systems

It seems likely that the Jahn–Teller distortions play an important role in helping the guest Cu²⁺ complexes accommodate to the geometry of the NH₄Cl host lattice. Our calculations suggest that the main contribution to the ground-state splitting stems from the linear Jahn–Teller coupling, while ligand strain [tetragonal Cl₄L₂ coordination (L = NH₃, H₂O)] and higher-order vibronic coupling contribute only to a minor extent. The Cu–Cl spacings of 274 pm that will occur for centers II and III if substitution occurs without distortion of the host lattice³⁷ are much larger than the value (259 pm) expected for a regular CuCl₆⁴⁻ octahedron.³⁸ Though many metal ions such as Co²⁺, Ni²⁺,^{13,39} and VO²⁺⁴⁰ form centers in CsCl-type lattices, high doping concentrations occur only for Mn²⁺^{41,42} and Cu²⁺. In the case of Mn²⁺ the large ionic radius (Mn–Cl = 268 pm)³⁸ means that this metal is of about the right size to occupy an interstitial facial site as far as the metal–halide distances are concerned, while with Cu²⁺ it is mainly the Jahn–Teller distortion—supported by the geometric effect of the different ligands—that makes the guest complex fit the requirements of the host lattice.

The nature of the distortion is decided by the interplay between the nonlinear vibronic interaction, represented by A₂ and β, which tends to cause an elongated tetragonal geometry, and inequivalence of the ligands, which favors a compressed tetragonal geometry. While for large –S₀/β ratios (center II, 12; center III, 6) the tendency to adopt a compressed coordination predominates, a compromise between compression and elongation, namely an orthorhombic geometry, is observed for center I where –S₀/β ≈ 2.

The temperature dependence of the *g* tensor of Cu(H₂O)₂Cl₄²⁻ has certain features in common with those reported for the Cu(H₂O)₆²⁺ ion doped into various host lattices. When the latter complex is doped into Zn(H₂O)₆SiF₆, a lattice with effectively regular octahedral host sites, a tetragonal *g* tensor is observed at low temperature, with a relatively sharp transition to an isotropic EPR signal occurring as the temperature is raised above ~20 K.²⁵ When Cu(H₂O)₆²⁺ is doped into K₂Zn(H₂O)₆(SO₄)₂, a site producing an orthorhombic lattice perturbation, an orthorhombic *g* tensor occurs at low temperature, which undergoes a gradual change toward tetragonal symmetry as the temperature is raised toward 300 K.^{16,43} The former behavior is due to exchange between three essentially equivalent wells in the potential surface, which is slow below ~20 K but fast above this temperature. The latter behavior is characteristic of three inequivalent wells in the potential surface, with the two lower wells being quite close in energy. At low temperature just the lowest well is populated, and this is characterized by an orthorhombic *g* tensor. As the temperature rises, thermal population of the slightly higher well occurs, and rapid exchange between these makes the *g* tensor tend toward axial symmetry (this would be achieved at a temperature sufficiently high to produce essentially equal population of the two wells). The complex Cu(H₂O)₂Cl₄²⁻ shows an orthorhombic *g* tensor at low temperature, which undergoes a comparatively sharp transition to a tetragonal signal with increasing temperature. The present interpretation suggests that in this system two wells in the Mexican hat potential surface with orthorhombic symmetries dominate the EPR parameters. Unlike the Cu²⁺ centers in K₂Zn(H₂O)₆(SO₄)₂, these lower wells are equal in energy (except for the effects due to random lattice strains), so that the orthorhombic–tetragonal transition in the EPR parameters occurs at low temperature and over a narrower temperature range than in

(35) Clayton, W. R.; Meyers, E. A. *Cryst. Struct. Commun.* **1976**, *5*, 61.

(36) Clayton, W. R.; Meyers, E. A. *Cryst. Struct. Commun.* **1976**, *5*, 63.

(37) These distances may be calculated from the lattice dimension *a* = 387.42 pm at 296 K reported by Boiko: Boiko, A. A. *Sov. Phys. Crystallogr. (Engl. Transl.)* **1970**, *14*, 539.

(38) Shannon, R. D.; Prewitt, C. T. *Acta Crystallogr., Sect. B: Struct. Crystallogr. Cryst. Chem.* **1969**, *B25*, 925 (estimated for a coordination number of 8 using an ionic radius of 1.86 Å for Cl[–]).

(39) Zaripov, M. M.; Chirkin, G. K. *Sov. Phys.—Solid State (Engl. Transl.)* **1965**, *7*, 74.

(40) Sastry, M. D.; Venkateswarlu, P. *Mol. Phys.* **1967**, *13*, 161.

(41) Heming, M.; Remme, S.; Lehmann, G. *J. Magn. Reson.* **1986**, *69*, 134.

(42) Bramley, R.; Starch, S. J. *Chem. Phys. Lett.* **1981**, *79*, 183.

(43) Silver, B. L.; Getz, D. *J. Chem. Phys.* **1974**, *61*, 638.

Cu²⁺-doped K₂Zn(H₂O)₆(SO₄)₂.

The behavior of the *g* tensors of the complexes Cu(NH₃)₂Cl₄²⁻ and Cu(NH₃)(H₂O)Cl₄²⁻ is quite similar to that reported for the CuF₆⁴⁻ ion doped into Ba₂ZnF₆⁴⁴ and K₂ZnF₄.¹⁵ All four species have axially symmetric *g* tensors, suggesting compressed tetragonal ligand coordination geometries, but while Cu(NH₃)₂Cl₄²⁻ and Cu²⁺-doped Ba₂ZnF₆ have *g*_{||} values very close to that expected for an electron in a pure d_{z²} orbital and EPR parameters that vary very little with temperature, Cu(NH₃)(H₂O)Cl₄²⁻ and Cu²⁺-doped K₂ZnF₄ both have *g*_{||} shifted substantially from the expected value, with this deviation increasing as the temperature is raised. Apparently, the two former species have potential surfaces with steep minima, while the two latter have potential surfaces that rise only slightly in energy as the ligands move from a tetragonal to an orthorhombic arrangement. An important distinction between the species in Cu²⁺-doped NH₄Cl and those in the above Zn²⁺ host lattices is that the anisotropy of the bond strengths causing the perturbation of the basic warped Mexican hat potential surface of each system is due to different ligands in the former case but to host lattice packing effects in the latter. Perhaps the most pleasing feature of the present model is that in every case the perturbation deduced from the behavior of the EPR parameters has been found to agree with the expectations of simple bonding theory and with the structural properties of the host lattices.

It would clearly be of interest to try to interpret the behavior of the centers formed when Cu²⁺ is doped into NH₄Br by using the present model, for comparison both with the results of Sorokin

(44) Friebel, C.; Propach, V.; Reinen, D. *Z. Naturforsch., B: Anorg. Chem., Org. Chem.* 1976, 31B, 1574.

and Chirkin¹⁸ and with those of the NH₄Cl systems, and a study of this kind is under way in our laboratories. However, the increased covalency and large spin-orbit coupling constant of the halide are expected to complicate the interpretation of the *g* values of the bromide complexes. The present results confirm other work^{26,45,46} which suggests that fluxional behavior due to vibronic coupling is a fairly common feature of copper(II) chemistry. It has even recently been shown that certain copper(II) complexes of biological importance have temperature-dependent EPR parameters indicative of dynamic structural changes,⁴⁷ and it was suggested that this might play a role in their biological activity. It may be noted that the simplest means by which dynamic behavior may be detected is via the temperature dependence of the EPR spectrum,⁴⁸ while the electronic spectrum will generally be rather insensitive to fluxional behavior of the kind discussed here.

Acknowledgment. We are grateful to the Humboldt Foundation for financial support to M.A.H., while M.J.R. and G.S. acknowledge the receipt of a Commonwealth Scholarship and a grant from the "Deutsche Forschungsgemeinschaft", respectively.

Registry No. *trans*-Cu(H₂O)₂Cl₄²⁻, 20102-44-7; *trans*-Cu(NH₃)₂Cl₄²⁻, 114027-34-8; *trans*-Cu(H₂O)(NH₃)Cl₄²⁻, 113859-50-0; Cu²⁺, 15158-11-9; NH₄Cl, 12125-02-9.

(45) Hathaway, B. J. *Struct. Bonding (Berlin)* 1984, 57, 55.

(46) Bersuker, I. B. *The Jahn-Teller Effect and Vibronic Interactions in Modern Chemistry*; Plenum: New York, 1984.

(47) Bacci, M.; Cannistraro, S. *Chem. Phys. Lett.* 1987, 133, 109.

(48) Chaudhuri, P.; Oder, K.; Wieghardt, K.; Weiss, J.; Reedijk, J.; Hinrichs, W.; Wood, J.; Ozarowski, A.; Stratemeier, H.; Reinen, D. *Inorg. Chem.* 1986, 25, 2951.

(49) Van der Valk, P. J.; Trappeniers, N. J. *Chem. Phys. Lett.* 1977, 52, 255.

Contribution from the Istituto per lo Studio della Stereochimica ed Energetica dei Composti di Coordinazione del CNR, via J. Nardi 39, Firenze, Italy, and Department of Chemistry, University of Florence, Firenze, Italy

X α -SW Calculations of the Electronic Structure and Magnetic Properties of Exchange-Coupled Transition-Metal Clusters. 2.¹ μ -Carbonato-Bridged Copper(II) Dimers

Carlo Albonico and Alessandro Bencini*

Received July 8, 1987

Symmetrically bridged (μ -carbonato)dycopper(II) complexes are diamagnetic and constitute one of the few examples of diamagnetic copper(II) dimers bridged by polyatomic groups. The self-consistent-field multiple-scattering X α model has been applied to calculate the magnetic coupling constant, *J*, of these complexes with the aim of explaining the origin of the observed diamagnetism. A singlet-triplet splitting of ≈ 4000 cm⁻¹ has been computed and has been related to a strong covalent interaction between the metal d orbitals and p orbitals of the carbonato oxygens with negligible contribution from the carbon atom. The magnetic behavior of other carbonato-bridged copper(II) complexes has been related to their geometrical structure by using an empirical orbital model.

Introduction

The understanding of the orbital mechanisms that determine the isotropic magnetic interaction between the ions forming transition-metal clusters is an actual topic that is attracting the interest of both chemists and physicists.¹⁻³ At the present stage of knowledge a number of experimental techniques, ranging from the measurement of the temperature dependence of magnetic susceptibility to optical spectroscopy and magnetic resonance techniques, allow one to measure also feeble interactions,³⁻⁶ and several quantum mechanical models can be used to relate the observed interactions to bonding and geometrical parameters.⁷⁻¹²

The effect of the isotropic exchange interaction on the energy levels of the cluster is generally represented through the spin Hamiltonian

$$H_{ex} = \sum_{a,b} J_{ab} S_a \cdot S_b \quad (1)$$

where the sum runs over all the neighboring paramagnetic metal atoms with total spin *S_i*, and *J_{ab}* is the exchange coupling constant between atoms *a* and *b*, which is evaluated experimentally.¹³

(1) Part 1: Bencini, A.; Gatteschi, D. *J. Am. Chem. Soc.* 1986, 108, 5763.

(2) *Magneto-Structural Correlations in Exchange Coupled Systems*; Willett, R. D., Gatteschi, D., Kahn, O., Eds.; D. Reidel: Dordrecht, The Netherlands, 1985.

(3) Carlin, R. L.; Duynveldt, A. J. *Magnetic Properties of Transition Metal Compounds*; Springer Verlag: New York, 1977.

(4) O'Connor, C. J. *Prog. Inorg. Chem.* 1982, 29, 203.

(5) Day, P. *Acc. Chem. Res.* 1979, 12, 203.

(6) Gatteschi, D. In *The Coordination Chemistry of Metalloenzymes*; Bertini, I., Drago, R. S., Luchinat, C., Eds.; D. Reidel: Dordrecht, The Netherlands, 1983; p 215.

(7) Anderson, P. W. *Phys. Rev.* 1959, 115, 2.

(8) Anderson, P. W. In *Magnetism*; Rado, G. T., Suhl, E. H., Eds.; Academic: New York, 1963.

(9) Bencini, A.; Gatteschi, D. *Inorg. Chim. Acta* 1978, 31, 11.

(10) Hay, P. J.; Thibault, J. C.; Hoffmann, R. *J. Am. Chem. Soc.* 1975, 97, 4884.

(11) Kahn, O.; Briat, B. *J. Chem. Soc., Faraday Trans. 2* 1976, 72, 268.

(12) Kahn, O.; Briat, B. *J. Chem. Soc., Faraday Trans. 2* 1976, 72, 1441.

(13) Ginsberg, A. P. *Inorg. Chim. Acta, Rev.* 1971, 5, 45.

* To whom correspondence should be addressed. Present address: Department of Chemistry, University of Florence, Florence, Italy.